Petrography and mineral chemistry of Escalón meteorite, an H4 chondrite, México

Adela M. Reyes-Salas[1,*], Gerardo Sánchez-Rubio[1], Patricia Altuzar-Coello[2], Fernando Ortega-Gutiérrez[1], Daniel Flores-Gutiérrez[3], Karina Cervantes-de la Cruz[1], Eugenio Reyes[4], and Carlos Linares[5]

*[1] Universidad Nacional Autónoma de México, Instituto de Geología,
Del. Coyoacán, 04510 México D.F., Mexico.*
*[2] Universidad Nacional Autónoma de México, Centro de Investigación en Energía,
Campus Temixco, Priv. Xochicalco s/n, 62580 Temixco Morelos, Mexico.*
*[3] Universidad Nacional Autónoma de México, Instituto de Astronomía,
Del. Coyoacán, 04510 México D.F., Mexico.*
*[4] Universidad Nacional Autónoma de México, Facultad de Química,
Del. Coyoacán, 04510 México D.F., Mexico.*
*[5] Universidad Nacional Autónoma de México, Instituto de Geofísica,
Del. Coyoacán, 04510 México D.F., Mexico.*
* adelars@servidor.unam.mx

ABSTRACT

The Escalón meteorite, a crusted mass weighing 54.3 g, was recovered near Zona del Silencio in Escalón, state of Chihuahua, México. The stone is an ordinary chondrite belonging to the high iron group H, type 4. Electron microprobe analyses of olivine ($Fa_{18.1}$) and pyroxene ($Fs_{16.5}$), phosphate, plagioclase, opaque phases, matrix and chondrule glasses are presented. The metal phases present are kamacite (6.08 % Ni), taenite (31.66 % Ni), high nickel taenite (50.01 % Ni) and traces of native Cu. The chondrules average apparent diameter measures 0.62 mm. X-ray diffraction pattern shows olivine, pyroxene and kamacite. Alkaline-type glass is found mainly in chondrules. This meteorite is a stage S3, shock-blackened chondrite with weathering grade W0.

Key words: chondrite, H4 type, electron microprobe analyses, Chihuahua, México.

RESUMEN

La meteorita Escalón, una roca con corteza de fusión de 54.3 g de peso, se recuperó cerca de la Zona del Silencio en el poblado de Escalón, Estado de Chihuahua, México. La roca es una condrita ordinaria que por su alto contenido en fierro pertenece al grupo H. Se realizaron análisis con microsonda electrónica, obteniendo olivino ($Fa_{18.1}$) y piroxena ($Fs_{16.5}$). Otros minerales analizados son fosfatos, plagioclasa, fases opacas y vidrios, tanto en matriz como en condros. Las fases metálicas presentes son kamacita (6.08 % Ni), taenita (31.66 % Ni), tetrataenita (50.01 % Ni) y trazas de cobre nativo. Con difracción de rayos X se identificaron los minerales olivino, piroxena, plagioclasa, troilita, y metales de

Fe-Ni. El promedio del diámetro aparente de los condros es de 0.62 mm. El vidrio es de tipo alcalino y se encuentra principalmente en condros. Los patrones de difracción de rayos X muestran la presencia de olivino, piroxena y kamacita. El estado de metamorfismo de choque en Escalón es S3 y el grado de intemperismo es W0.

Palabras clave: condrita, H4, metamorfismo, microsonda electrónica, Chihuahua, México.

INTRODUCTION

Meteorites recovered following observed falls are called *falls;* those which can not definitely be associated with observed falls are called *finds.* Based on their bulk compositions and textures, meteorites can be divided into two major categories *chondrites* and *achondrites or nonchondritic meteorites;* the latter include the *primitive achondrites* and *igneously differentiated meteorites* (Krot *et al.,* 2003). Chondrites are broadly ultramafic in composition, consisting largely of iron, magnesium silicon and oxygen. The most abundant constituents of chondrites are chondrules, which are igneous particles that crystallized rapidly in minutes to hours. They are composed largely of olivine and pyroxene, commonly contain metallic Fe Ni, are 0.01–10 mm in size and are rounded (Scott and Krot, 2003).

The primary divisions of chondrite classification include the carbonaceous (C), ordinary (O) and enstatite (E) classes, each of which contains distinct groups that are closely related. The O class is divided into three groups, H, L and LL. H chondrites have high total Fe content, L chondrites have low total Fe content, and LL chondrites have low metallic Fe relative to total Fe, as well as low total Fe content.

A classification scheme that identifies the degree and nature of secondary alteration (petrologic type) experienced by a chondrite was introduced by Van Schmus and Wood (1967). In this scheme, type 3 is the least altered material, types 2 to 1 represent increasing degrees of aqueous alteration and types 4 to 6 represent increasing degrees of thermal metamorphism (Brearley and Jones, 1998).

The degree of shock metamorphism recorded in a chondrite is determined from a variety of mineralogical and textural parameters. Stöffler *et al.* (1991) defined increasing shock stages of S1 to S6 for ordinary chondrites. An additional classification parameter is used to identify the degree of terrestrial weathering that a chondrite has experienced; Wlotzka (1993) suggested progressive alteration stages, based on features in polished sections, from W0 to W6.

One piece of Escalón meteorite was found in 1979 by Dr. Luis Maeda Villalobos in the surroundings of the Escalón railroad station, which is located in southern Chihuahua, northern México at 26°45' N, 104°20' W (Sánchez-Rubio *et al.*, 2001) (Figure 1). This unique and
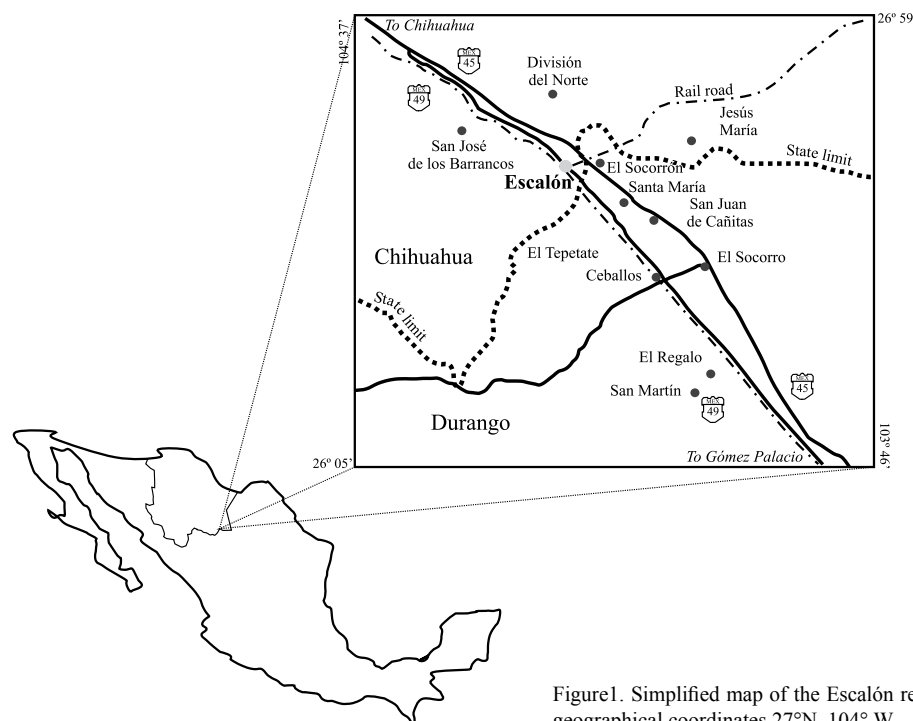

Figure1. Simplified map of the Escalón region, Chihuahua, with geographical coordinates 27°N, 104° W.

fresh looking piece shows an intact black fusion crust, which suggests that the stone did not suffer terrestrial weathering. It has a rounded shape and 54.3 grams in weight. The finder, Dr. Maeda, unfortunately, failed to search the area for others specimens. The fresh cut surface is black in color and, under the petrographic microscope, it shows an extremely unsorted pseudosedimentary material where chondrules form about 60 % of the whole mass and show well defined shapes, with size ranging up to 2 mm in diameter.

The name Escalón meteorite was submitted to the Nomenclature Committee of the Meteoritical Society, and the find as well as the classification of the stone as an H4 chondrite, were published in the Meteoritical Bulletin (Wlotzka, 1994).

The meteorite was classified as an ordinary chondrite H4, according to its chemical composition and petrography, following the scheme devised by Van Schmus and Wood (1967) (Sánchez-Rubio, *in* Wlotzka, 1994). The purpose of this paper is to present a detailed petrographic and mineralogic study to confirm the classification of the meteorite as H4. These data include studies of its texture and composition of main minerals. To complete this classification, schock stage (Stöffler *et al.*, 1991) and weathering grade (Wlotzka, 1993) were studied, indicating a slight shock stage of S3, and weathering grade W0.

ANALYTICAL PROCEDURES

Sample of Escalón were obtained by request from the Meteorite working group of Instituto de Geología, UNAM. X-ray diffraction analyses were obtained from bulk powders. One polished thin section was prepared and studied under the polarizing microscope. Quantitative analyses of minerals and glasses were performed on the polished thin section, using a JEOL superprobe 733 of the National Institute of Polar Research, Japan. A JEOL JXA-8900R with a quantitative wavelength-dispersive analyses and also a JEOL jsm 35c with a Tracor-Noran energy dispersive X-ray analysis system attached to the SEM, using natural and synthetic minerals as standards in the premises of the institutes of Geophysics and Geology, at the main campus of the Universidad Nacional Autónoma de México, in México City. Analyses were conducted at 20 keV accelerating potential with a probe current of 20 nA, a beam size of 1 μm and 10–40 s counting times. ZAF correction was made to all analytical data obtained. The polished thin section of the Escalón meteorite was also examined with scanning-electron microscopy (SEM) using back-scattered electron (BSE) image techniques. XRD analysis were performed on pulverized bulk rock samples. X-ray diffraction (XRD) were collected using a Siemens D5000 diffractometer (40 kV, 30 mA) with Cu Kα radiation ($\lambda_{K\alpha1}$ = 1.5406 Å, $\lambda_{K\alpha2}$ = 1.54439 Å), 2θ range between 20° and 70°, step size of 0.02 °2θ, 1.2 s/step, divergence slit = 0.5 mm, and receiving slit = 0.3 mm.

RESULTS

Petrography and mineral chemistry

Optical microscopy

The chondrite consists of chondrules (spherical or subspherical, commonly sub-milimetric petrographic objects that show evidence of a molten or partially molten origin), crystal fragments, and matrix (fine grained aggregates of material filling the interstices between chondrules and crystal fragments) (Figure 2). The identified mineral phases in Escalón are olivine, pyroxene, plagioclase, merrilite and chlorapatite as well as troilite, taenite, kamacite, chromite and pentlandite. Olivine, pyroxene, troilite, kamacite and taenite are the main constituents besides chondrules.

Olivine and pyroxene are the predominant silicates; minor plagioclase shows characteristic albite twinning. Olivine is resorbed and silicates show euhedral to anhedral shape, with common wavy extinction. There is no visible
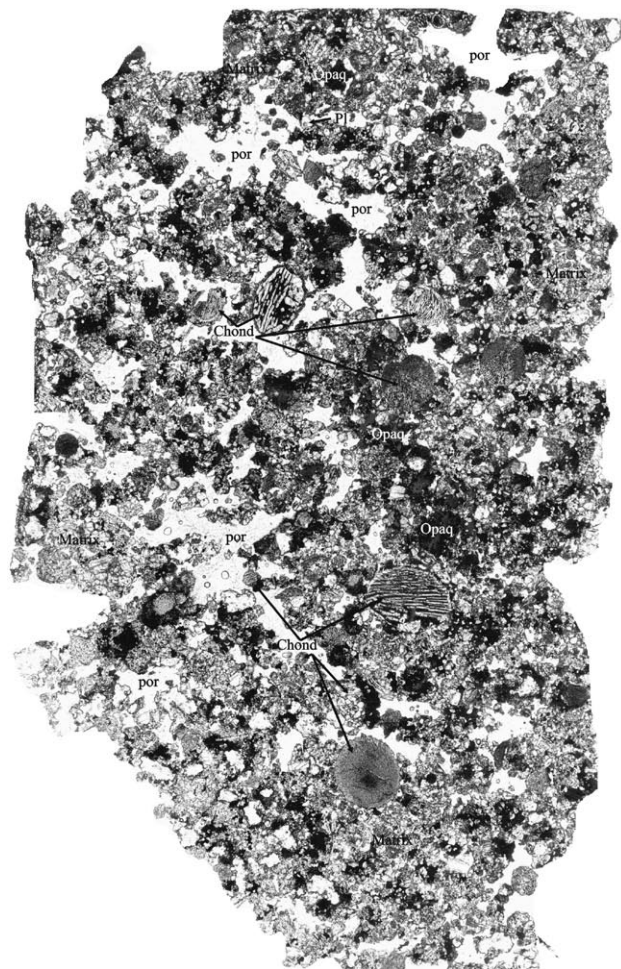

Figure 2. Phothomicrograph of the thin section of the Escalón meteorite showing large and distinct chondrules, as well as abundant opaque phases and silicates disseminated throughout the matrix. The section is about 2.4 cm across. Opaq: opaque minerals; por: pores; Chond: chondrule; Pl: plagioclase.

oxidation of metal or sulfide, and only a limonitic staining may be noticeable in transmitted light.

Electron microscopy

Olivine and pyroxene grains were analysed by electron microprobe to determine their compositions and degree of equilibration. Representative analyses are given in Tables 1 and 2. The composition is quite uniform; grains inside chondrules have the same composition as those outside chondrules. Olivine (34 analyses) with an average fayalite (Fa) content of 18.1 ± 0.4 mol %; low-Ca pyroxene (32 analyses) show an average ferrosilite (Fs) content of 16.5 ± 0.35 mol %, whereas wollastonite content (Wo) in orthopyroxene is 1.5 ± 0.2 mol %; the average composition of four high-Ca pyroxene grains is Wo 41.7 ± 2.7 mol %. This composition is similar to most analyses in the H group range (Scott *et al.*, 1986; Brearley and Jones, 1998).

Pyroxenes are mainly orthopyroxene, but less than 5% of the grains are clinopyroxene with $Wo_{41.7}$ (% mol), which is similar to diopside composition. Growth steps are visible on the faces of olivine and pyroxene crystals. Other minerals identified in the polished thin section are pentlandite, merrilite, chlorapatite, native copper as inclusion in taenite, and tetrataenite.

Plagioclase occurs in the matrix, with composition $Ab_{85.2 \pm 1.1}$, $An_{12.8 \pm 1.3}$, $Or_{5 \pm 0.5}$ (Table 3), which is near the mean equilibrated H chondrite plagioclase composition (Van Schmus and Ribbe, 1968).

Chloroapatite and merrilite are common accessory minerals in equilibrated ordinary chondrites and they usually occur interstitially among ferromagnesian silicates in the matrix and associated with metal and sulphide phases (Yabuki and Goresy, 1986).

The phosphates in Escalón are mostly merrillite and up to 200 μm in size; merrillite was found in the matrix associated with kamacite, troilite and chromite; it was also found as relatively large crystals in the groundmass of barred olivine chondrule (Figure 3a) and as crystals attached to the surface of chondrules. Merrillite is also mixed with chlorapatite (Figure 3b).

Opaque minerals make up less than 20% of the meteorite, with troilite more abundant than Fe-Ni grains and minor chromite, merrillite, pentlandite and copper metal.

Chromite crystals are frequent. The composition of chromite (Table 4) shows a Fe/(Fe+Mg) of 0.847 ± 0.03,

Table 1. Representative electron microprobe analyses (wt. %) and calculated cations of olivine.

	J1	J2	J6	J15	J16
SiO_2	38.86	38.93	38.78	39.08	39.13
TiO_2	0.06	0.00	0.00	0.01	0.04
Al_2O_3	0.00	0.00	0.06	0.00	0.00
Cr_2O_3	0.00	0.00	0.00	0.00	0.00
FeO	16.82	17.39	16.55	17.23	16.93
MnO	0.22	0.39	0.52	0.33	0.39
MgO	43.39	43.31	42.77	43.67	43.28
NiO	0.00	0.00	0.00	0.00	0.00
CaO	0.03	0.05	0.01	0.01	0.00
Total	99.380	100.070	98.69	100.33	99.77
Cations calculated on the basis of four oxygens					
Si	0.992	0.990	0.996	0.990	0.995
Ti	0.001	0.000	0.000	0.000	0.001
Al	0.000	0.000	0.002	0.000	0.000
Cr	0.000	0.000	0.000	0.000	0.000
Fe(ii)	0.359	0.370	0.356	0.365	0.360
Mn	0.005	0.008	0.011	0.007	0.008
Mg	1.651	1.642	1.638	1.649	1.640
Ni	0.000	0.000	0.000	0.000	0.000
Ca	0.001	0.001	0.000	0.000	0.000
Total	3.008	3.011	3.003	3.011	3.004
Endmembers					
Forsterite	81.9	81.500	81.7	81.7	81.7
Fayalite	18.0	18.5	18.3	18.3	18.3

Table 2. Representative electron microprobe analyses (wt. %) and calculated cations of orthopyroxene and clinopyroxene.

	J5	J7	J8	J19	J23	L5	L7
SiO_2	56.00	56.00	56.05	56.11	55.29	53.48	53.50
TiO_2	0.16	0.09	0.24	0.16	0.17	0.50	0.00
Al_2O_3	0.17	0.06	0.18	0.13	0.22	0.64	0.17
Cr_2O_3	0.10	0.15	0.31	0.17	0.16		1.20
FeO	11.22	10.77	10.75	10.26	10.71	3.46	4.07
MnO	0.43	0.87	0.60	0.19	0.53	0.17	0.26
MgO	32.07	31.87	31.61	31.33	31.04	17.88	17.47
CaO	0.66	0.87	0.60	0.66	0.87	21.77	22.47
Na_2O	0.04	0.08	0.00	0.00	0.02	0.63	0.01
K_2O	0.03	0.00	0.02	0.00	0.00	0.00	0.02
Total	100.88	100.76	100.36	99.01	99.01	98.52	99.16
Cations calculated on the basis of six oxygens							
Si	1.965	1.969	1.973	1.992	1.974	1.965	1.976
Ti	0.004	0.002	0.006	0.004	0.005	0.014	0.000
Al	0.007	0.002	0.007	0.005	0.009	0.028	0.007
Cr	0.003	0.004	0.009	0.005	0.005	0.000	0.035
Fe(II)	0.329	0.317	0.316	0.305	0.320	0.106	0.126
Mn	0.013	0.026	0.018	0.006	0.016	0.005	0.008
Mg	1.678	1.670	1.659	1.658	1.652	0.980	0.962
Ca	0.025	0.033	0.023	0.025	0.033	0.857	0.889
Na	0.003	0.005	0.000	0.000	0.001	0.045	0.001
K	0.001	0.000	0.001	0.000	0.000	0.000	0.001
Total	4.028	4.028	4.013	3.999	4.015	4.000	4.004
Fe(II)	0.244	0.230	0.277	0.307	0.273	0.047	0.114
Fe(III)	0.083	0.085	0.038	-0.003	0.045	0.059	0.012
$Fe^2/(Fe^2+Fe^3)$	0.747	0.730	0.879	1.009	0.858	0.442	0.904
$Fe^3/(Fe^3+Fe^2)$	0.253	0.270	0.121	-0.009	0.142	0.558	0.096
Endmembers							
Wollastonite	1.2	1.6	1.1	1.3	1.6	43.01	44.8
Enstatite	82.0	81.5	82.3	83.2	81.7	49.15	48.4
Ferrosilite	16.6	16.6	16.5	15.6	16.6	5.57	6.7
Acmite	0.1	0.3	0.0	0.0	0.1	2.26	0.0

Table 3. Representative electron microprobe analyses (wt. %) and calculated cations of plagioclase.

	L8	L9	L10	L11	L12
SiO_2	63.95	64.34	65.26	65.12	64.34
Al_2O_3	22.80	20.80	21.19	21.47	20.80
FeO	0.85	0.53	0.25	0.35	0.53
CaO	2.62	2.84	2.26	2.17	2.84
Na_2O	8.22	9.55	9.04	8.77	9.55
K_2O	0.81	0.80	0.96	0.79	0.80
Total	99.25	98.85	98.96	98.67	98.85
Cations calculated on the basis of 32 oxygens					
Si	2.839	2.881	2.901	2.897	2.881
Al	1.193	1.097	1.110	1.126	1.097
Tot Fe^{+2}	0.032	0.020	0.009	0.013	0.020
Ca	0.125	0.136	0.108	0.103	0.136
Na	0.707	0.828	0.779	0.757	0.828
K	0.046	0.045	0.055	0.045	0.045
Total	4.941	5.008	4.961	4.941	5.008
Endmembers					
Albite	80.6	82.0	82.7	83.6	82.0
Anorthite	14.2	13.5	11.5	11.4	13.5
Orthoclase	5.2	4.5	5.8	4.9	4.5

which is within the range of those reported for H chondrites (Bunch *et al.*, 1967; Nehru *et al.,* 1997).

The chromite forms individual anhedral to subhedral grains, 20-100 μm in size, isolated from other opaque phases or close to metals and troilite. Also, there are local aggregates up to 300 μm, associated with plagioclase glass (Figures 3c, 3d) and similar to CPA (chromite-plagioclase assemblages) of Rubin (2003). Chromite in Escalón meteorite also occurs as small inclusions (blebs) <3 μm in chondrules and in olivine crystals (Figure 3f).

A few mafic silicate grains in Escalón contain Fe-Ni blebs (Figure 3e) and small chromite blebs (Figure 3f). Similar chromite blebs have been reported in shocked ordinary chondrite (Rubin, 1992).

Modal analysis, based on 300 points counts on an area of a thin section by using SEM-EDS thechnique, were obtained for metals and sulfides, showing the following values: troilite 52 %; kamacite 35 %; taenite 10 %; tetrataenite 3 % and scarce native copper and pentlandite.

Kamacite can be observed on large grains up to 1 mm in diameter, as tiny granules (1–5 μm) inside some chondrules and also in the matrix. The larger grains have irregular margins and some of them present growth steps typical of group H chondrite (Michel-Levy, 1981), and perhaps it also contains olivine inclusions (Figure 4a), or other opaque phases such as native copper (Figures 4b, 4c).

The average cobalt concentration in kamacite is 0.318–0.432 wt. %. The results for Ni and Co are similar to other H group meteorites.

Taenite is present in less proportion that kamacite and tends to form slightly smaller grains, in places associated

with troilite, kamacite and tetrataenite (Figures 4d, 4e, 4f). Ni-rich zones known as clear taenite (tetrataenite) that surround taenite display a characteristic M-shaped (Wood, 1967; Clarke and Scott, 1980) Ni concentration profile, with the highest Ni content concentrated at the edge (± 50 wt%), and the lowest in the center (± 30 wt. %). Tetrataenite occurs as grains of 5–50 μm, some also as rims 1–20 μm wide on taenite grains (Figures 4e, 4f) and in places with troilite grain inclusions. In Escalón meteorite, kamacite and taenite also occur intergrown, forming the phase plessite (Figures 4d, 4f) (Brearley and Jones, 1998).

Troilite is more abundant than metal grains and can be seen with sizes of 10–200 μm. It is associated with metal and chromite grains and also occurs inside metal grains. Representative analyses of Fe-Ni and troilite are given in Tables 5 and 6.

Scanning electron images were obtained from grains of opaque phases in the Escalón meteorite. Although some grains appear homogeneous, other show complex intergrowths of Ni-rich areas (Figure 4f).

Chondrules tend to show well defined boundaries. The measurement of the apparent diameters of about 50 chondrules showed an average of 0.62 mm and a range of

Table 4. Representative electron microprobe analyses (wt. %) and calculated cations of chromite.

|	ch1	ch2	ch6	ch7	ch8
SiO_2	0.067	0.011	0.295	0.023	0.007
TiO_2	2.002	1.752	1.833	2.008	1.823
Al_2O_3	7.191	6.732	6.988	6.600	6.364
Cr_2O_3	56.320	55.436	55.921	55.976	56.156
V_2O_3	0.000				
FeO	30.376	30.969	30.445	31.190	30.980
MnO	0.908	0.982	0.957	1.050	0.434
MgO	3.961	2.764	2.636	2.659	3.594
CaO	0.000	0.058	0.118	0.031	0.000
ZnO	0.000	0.000	0.000	0.000	0.000
Total	100.825	98.704	99.193	99.537	99.358
Cations calculated on the basis of 32 oxygens					
Si	0.019	0.003	0.084	0.007	0.002
Ti	0.420	0.379	0.393	0.431	0.391
Al	2.364	2.283	2.346	2.221	2.138
Cr	12.420	12.611	12.593	12.635	12.658
V	0.000	0.000	0.000	0.000	0.000
Fe(ii)	7.085	7.452	7.252	7.446	7.386
Mn	0.215	0.239	0.231	0.254	0.105
Mg	1.647	1.186	1.119	1.132	1.528
Ca	0.000	0.018	0.036	0.009	0.000
Zn	0.000	0.000	0.000	0.000	0.000
Total	24.169	24.171	24.054	24.135	24.209
Fe/Fe+Mg	0.811	0.863	0.866	0.868	0.829
Cr/Cr+Al	0.840	0.847	0.843	0.851	0.855
Fe(II)	6.587	6.947	7.092	7.048	6.771
Fe(III)	0.448	0.452	0.143	0.357	0.551
$Fe^2/(Fe^2+Fe^3)$	0.936	0.939	0.980	0.952	0.925
$Fe^3/(Fe^3+Fe^2)$	0.064	0.061	0.020	0.048	0.075
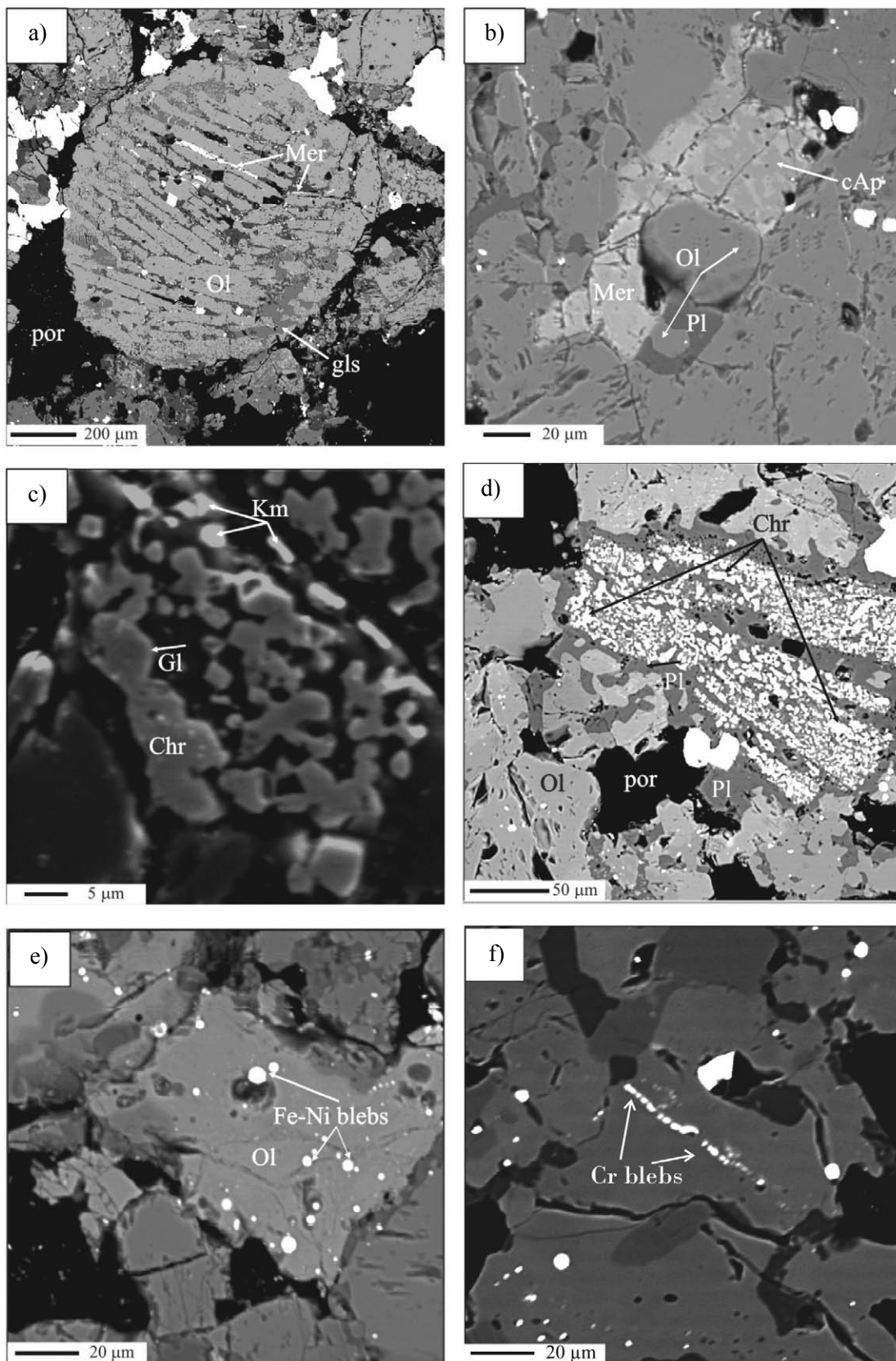
Figure 3. a: Backscattered image of merrillite as large crystals (up to 200 μm in size) inside the groundmass of a barred olivine chondrule; b: Merrillite is also mixed with chlorapatite. c and d: Chromite-bearing shock features as local aggregates up to 300 μm, associated with plagioclase glass or chromite-plagioclase assemblages (CPA); e: Fe-Ni blebs and small chromite veinlets; f: Chromite blebs in olivine grain. Chr= chromite, CPA= chromite-plagioclase assemblage, gls= glass in chondrule, Mer= merrillite, Ol= olivine, por= pores, Pl= plagioclase. 1.Gl= glass in CPA, cAp= clorapatite, Km= kamacite
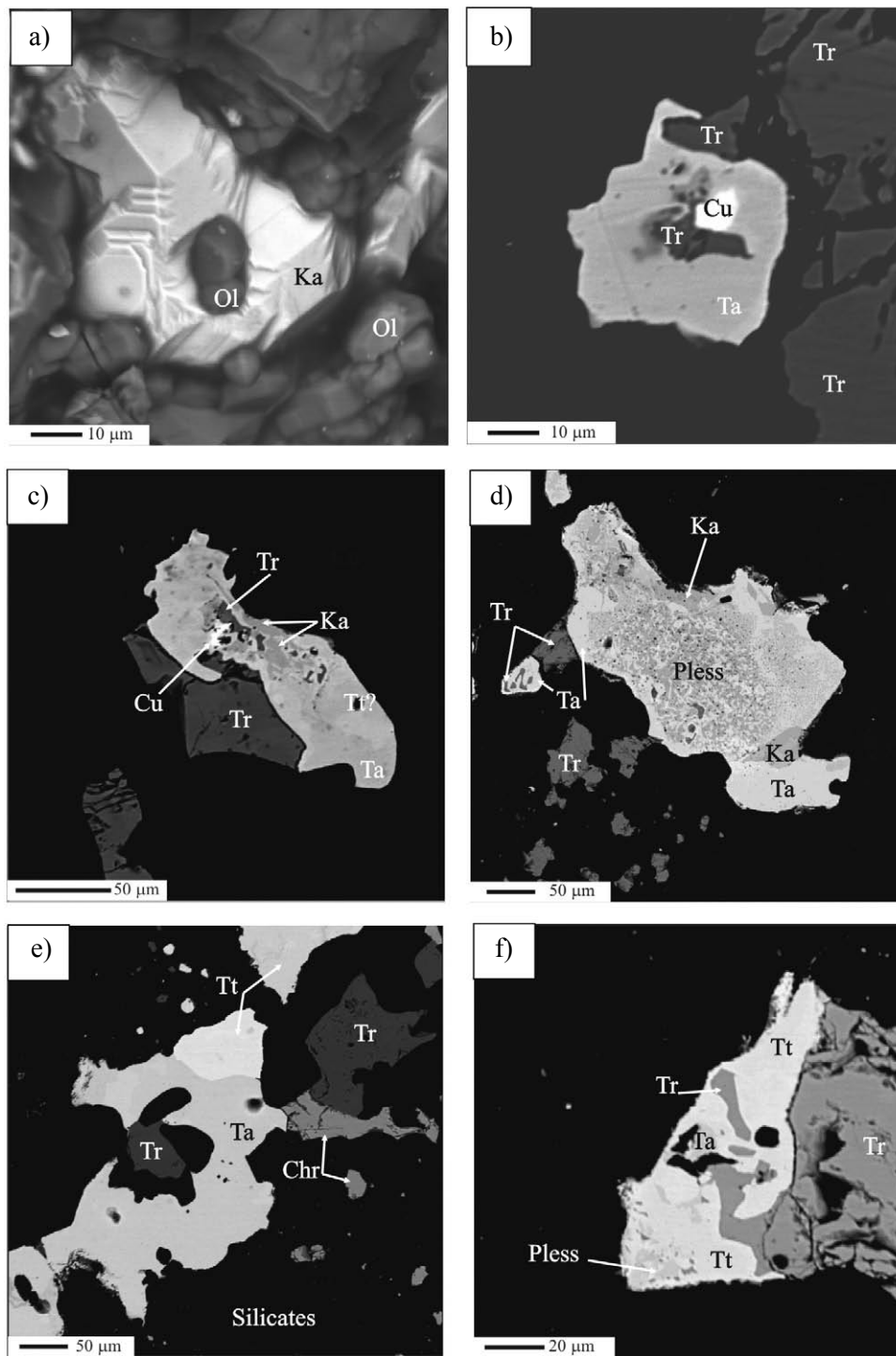
Figure 4. a: Backscattered image of kamacite with growth steps typical of group H chondrite shows geometrical planes, also contain olivine inclusion and euhedral olivine grains around kamacite. b, c: Backscattered electron images of metallic cupper, petrographic assemblage shows Cu enclosed in metal and near troilite grains; d, e: Tetrataenite as grains on taenite minerals; f: Fe-Ni with troilite grain inclusions, kamacite and taenite can observed as an intergrowth which is termed plessite. Chr= chromite, Cu= cupper, Ka= kamacite, Ol= olivine, Pless=plessite, Ta= taenite, Tr = troilite, Tt= tetrataenite.

0.23–2.25 mm apparent diameters. The mean diameter of 0.62 mm was larger than the normal for H chondrites (300 µm for H chondrites; Grossman *et al.*, 1988).

The chondrules are spherical or oval in shape, sometimes polysomatic (Figure 5a), often display rims of fine-grained olivine, pyroxene and opaque phases in a glass matrix (Figure 5b). Chondrules in the Escalón meteorite are of two main types: BO (barred olivine) (Figures 3a, 5 a, 5b, 6b, 6c, 7c, 7e, 7f) and RP (radial pyroxene) (Figure 6f). The BO chondrules may also have orthopyroxene combined

Table 5. Representative electron microprobe analyses (wt. %) of Fe-Ni phases.

	Ka-1	Ka-2	Ka-4	Ta-1	Ta-2	Ta-3	Tt-1	Tt-2	Tt-3
Fe	95.165	93.320	94.131	64.325	70.840	69.917	51.956	47.508	47.739
Ni	5.465	6.318	6.031	34.530	30.588	29.870	45.565	51.942	52.529
Co	0.432	0.327	0.318	0.131	0.135	0.144	0.103	0.050	0.065

Ka: kamacite; Ta: taenite; Tt: tetrataenite

with minor amounts of Fe-Ni metal grains distributed throughout the chondrule (Figure 7f). Some interstitial glass was also observed (Figure 7f). A readily distinguished porphyritic olivine and pyroxene (POP) chondrule, whith some olivine grains showing ondulatory extinction, is also present (Figure 5d).

Others chondrules were GO (granular olivine) with well-defined borders (Figure 6a); some are porphyritic (with

Table 6. Representative electron microprobe analyses (wt. %) of troilite.

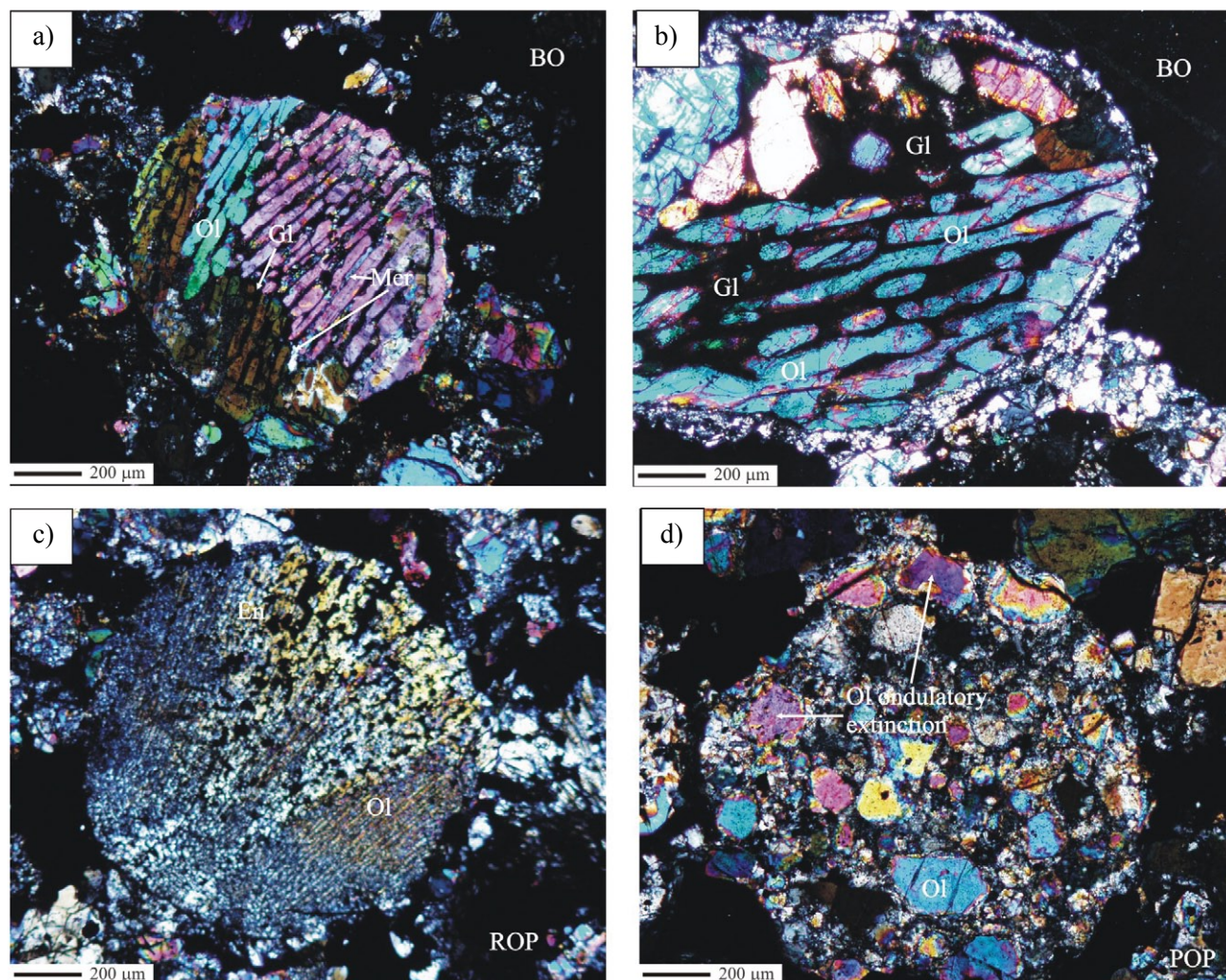|	Tr1	Tr2	Tr3
Fe	62.974	64.335	64.174
Co	0.051	0.019	0.037
S	35.729	35.663	35.806
Ni	0.101	0.002	0.020
Total	98.855	100.019	100.037

Figure 5. Photographs of chondrules, microscopic observations with crossed nicols. a: Barred olivine (BO) polysomatic chondrule composed of several parts with different crystallographic orientations of olivine bars and merrilite inclusions. b: BO chondrule with rims of fine-grained olivine, pyroxene and opaque phases in glass matrix. c: Radial olivine and pyroxene (ROP) chondrule with complex texture showing radial pyroxene and olivine texture of fine grains where the fibers grow in different orientations. d: Readily distinguished porphyritic olivine and pyroxene (POP) chondrule; some olivine grains with ondulatory extinction. BO= barred olivine, ROP= radial olivine and pyroxene, En= enstatite, Gl= glass, Mer= merrillite, Ol= olivine.
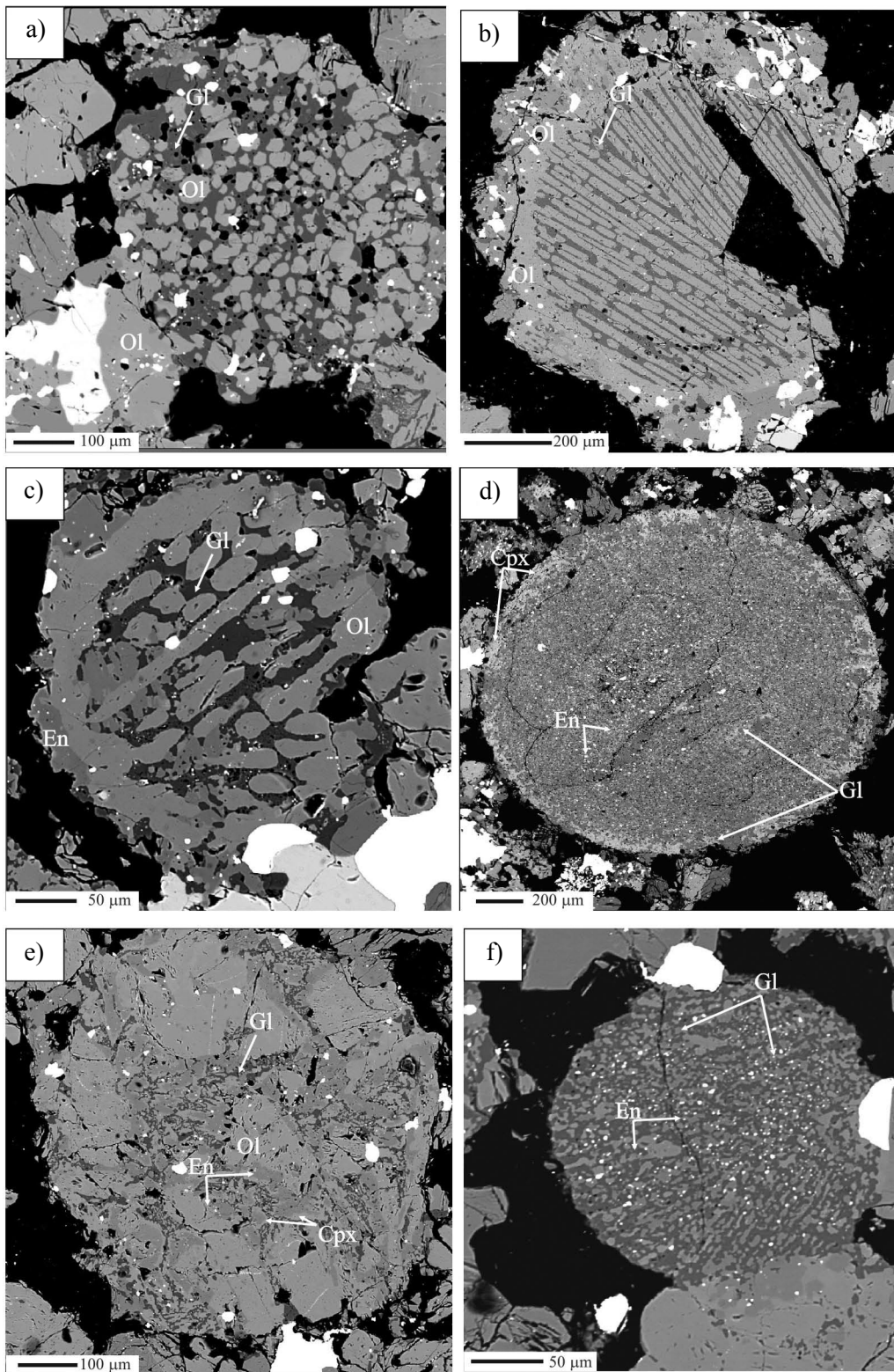
Figure 6. a: Granular olivine (GO) chondrule with well-defined borders. b: Barred olivine (BO) chondrules with olivine shell enclosing the chondrule. c: BO chondrule with a thick olivine shell. The olivine bars are discontinuous. d Cryptocrystalline chondrule with very fine laths of pyroxene, a small amount of Fe-Ni and glass; a thin rim of clinopyroxene grains surrounds this chondrule. e: Porphyritic olivine-pyroxene (POP) chondrule; crystals inside the chondrule are euhedral. f: Radial pyroxene (RP). CPx= clinopyroxene, En= enstatite, Gl= glass, Ol= olivine.
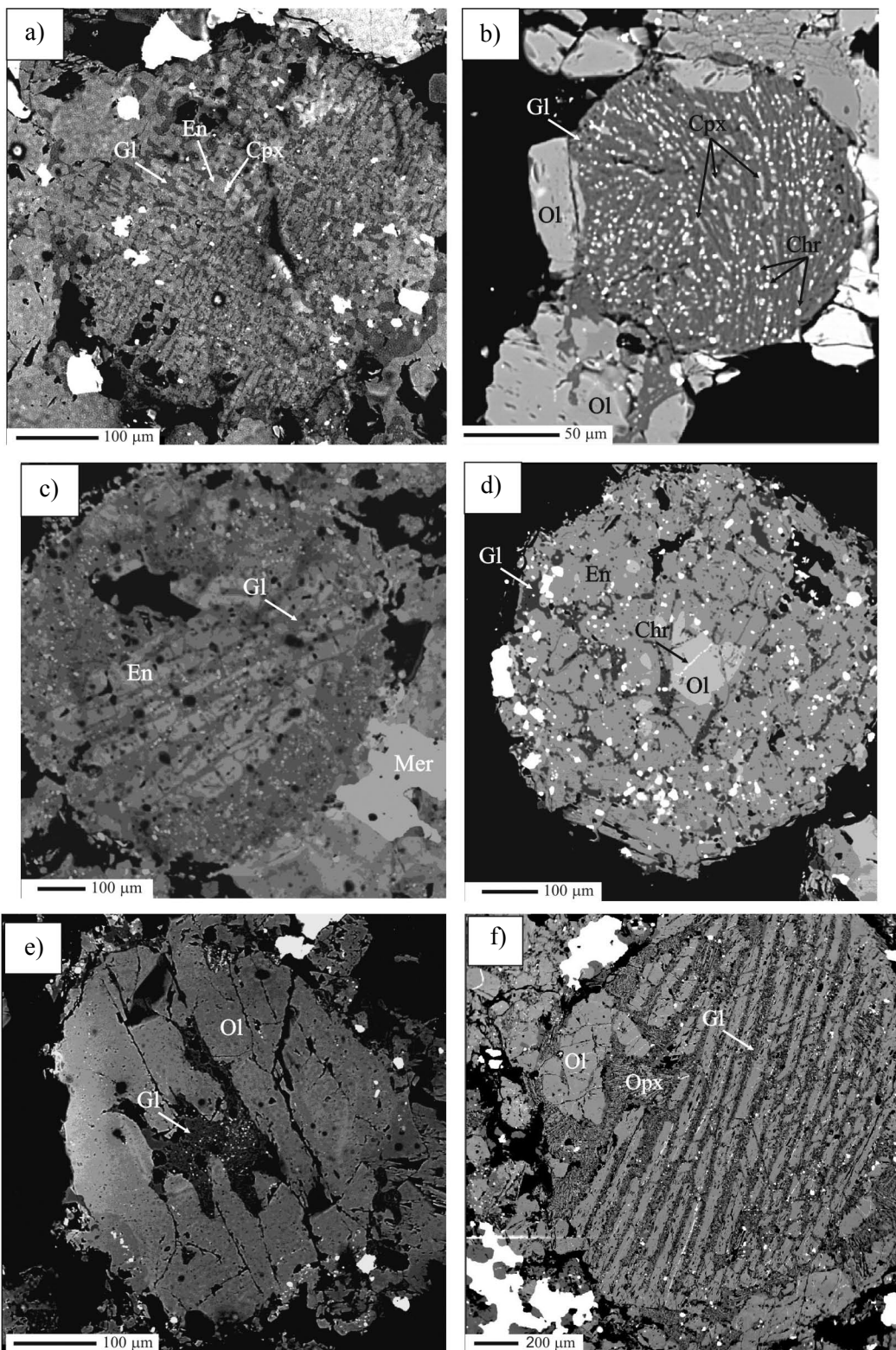
Figure 7. Chondrules in Escalón meteorite with unusual textures. a: Probably barred pyroxene (BP) with glass, bars present two different orientations; b: Unusual chondrule in the Escalón meteorite composed by radial and small grains of chromite and high-Ca-pyroxene; chondrule matrix has feldesphatic glass composition and to the right a conspicuous subhedral merrillite crystal is observed; c: barred olivine (BO) glass-rich chondrule with pores; d: Porphyritic chondrule composed of olivine and pyroxene (POP); at center discontinuous chromite veinlet within euhedral olivine surrounded by orthopyroxene grains some of which have olivine inclusions; e: BO chondrule, the groundmass center of this chondrule is mostly glassy; f: a transitional BO texture; outer zone on the left shows pyroxene radial texture. Cpx= clinopyroxene, Chr= chromite, En= enstatite, Gl= glass, Ol= olivine.

phenocrysts), a common texture termed POP (porphyritic chondrules composed of olivine and pyroxene) (Figure 6e), and finally some are C (cryptocrystalline) (Figure 6d). Apart from these typical petrological textures, other chondrules in Escalón show unusual textures such as probably barred pyroxene with glass (Figure 7a), a transitional texture BO with pyroxene radial texture (Figure 7f), Radial olivine and pyroxene (ROP) chondrules with a complex texture of radial olivine and pyroxene where the fine grained fibers grow in different orientations (Figure 5c). It includes an unusual matrix-rich chondrule with chromite and high-Ca pyroxene (Figure 7b), some glass-rich chondrules (Figure 7c, 7e), and one POP chondrule has a large central euhedral olivine crystal with a discontinuous chromite veinlet (possible restitic grain?), which is rimmed by orthopyroxene grains (Figure 7d).

Glass is found in chondrules (10–29 %) and in the matrix (~5 %). All analysed glasses (Table 7) are similar in composition and they are highly recrystallized in some instances. This glass is rich in Na, Al, and Ca, and poor in Fe and Mg. The glass analyses reveal an alkaline composition (Figures 8a, 8b). Normative mineralogy includes albite, anorthite, nepheline, orthoclase and corundum (Table 7).

Troilite, kamacite and chromite were identified also within the glass phase.

Table 7. Major element (wt. %) contents of representative glasses and their normative analyses.

	vidrio15	vidrio16	vidrio18	vidrio20	vidrio24
SiO_2	63.43	62.68	64.05	62.63	64.21
TiO_2	0.04	0.07	0.04	0.08	0.05
Al_2O_3	22.95	20.75	21.31	22.11	21.17
FeO	0.27	0.60	0.52	0.93	0.38
MnO	0.03	0.01	0.01	0.03	0.00
MgO	0.01	0.81	0.02	0.07	0.05
CaO	2.58	3.98	2.62	2.93	2.65
Na_2O	11.26	9.77	10.43	10.07	10.67
K_2O	0.12	0.13	0.22	0.20	0.18
SO_3	0.01	0.31	0.02	0.14	0.00
NiO	0.00	0.00	0.04	0.01	0.00
Total	100.68	99.12	99.28	99.19	99.37
CIPW norm					
or	0.68	0.79	1.31	1.17	1.08
ab	77.71	77.53	83.22	79.27	83.27
an	11.67	12.50	10.75	14.65	9.40
ne	9.14	3.31	3.08	3.64	4.10
C	0.00	0.00	0.12	0.00	0.25
di	0.04	4.41	0.87	0.00	1.39
wo	0.39	0.65	0.00	0.12	0.00
ol	0.00	0.00	0.00	0.00	0.00
mt	0.00	0.00	0.02	0.07	0.00
il	0.06	0.02	0.59	1.04	0.42
hem	0.30	0.68	0.05	0.01	0.09
pero	0.02	0.11	0.00	0.04	0.00

X-ray diffraction

X-ray diffraction (XRD) pattern recorded for Escalón samples are shown in Figure 9. The XRD pattern from the powdered sample shows three phases: pyroxenes (enstatite) (PDF 19-0768); olivine (forsterite) (PDF 34-0189); and iron (kamacite) (PDF 37-0474).

The most abundant mineral in Escalón is olivine (~50%), followed by pyroxene (enstatite) (~32 %), and iron (kamacite) (~18%). The semiquantitative analysis were estimated from the main peak intensity of each mineral phase: Olivine (forsterite) (d = 2.4567 Å), pyroxene (enstatite) (d = 2.8700 Å) and , iron (kamacite) (d = 2.0280 Å).

DISCUSSION

Based on olivine and low-Ca pyroxene composition, Escalón meteorite can be classified as an H group chondrite. The olivine and orthopyroxene compositions are within the range of the H chondrites (fayalite content of 18.1 mol %
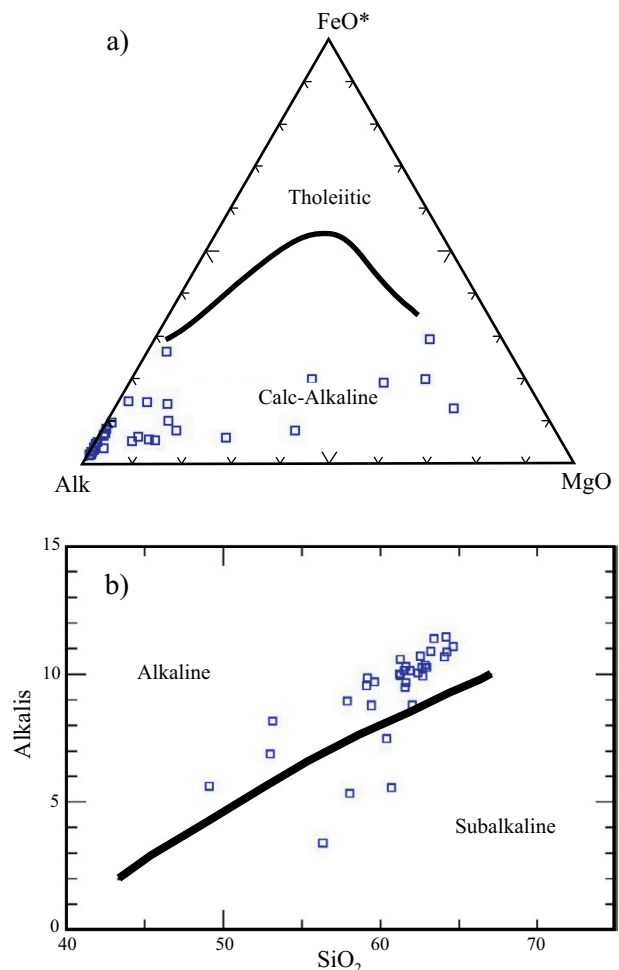

Figure 8. Composition of glass in chondrules and matrix of the Escalón meteorite in AFM and Alkalis (Na_2O+K_2O) *vs.* silica (Irvine and Baragar, 1971) diagrams. Alk: alkalis (Na_2O+K_2O).
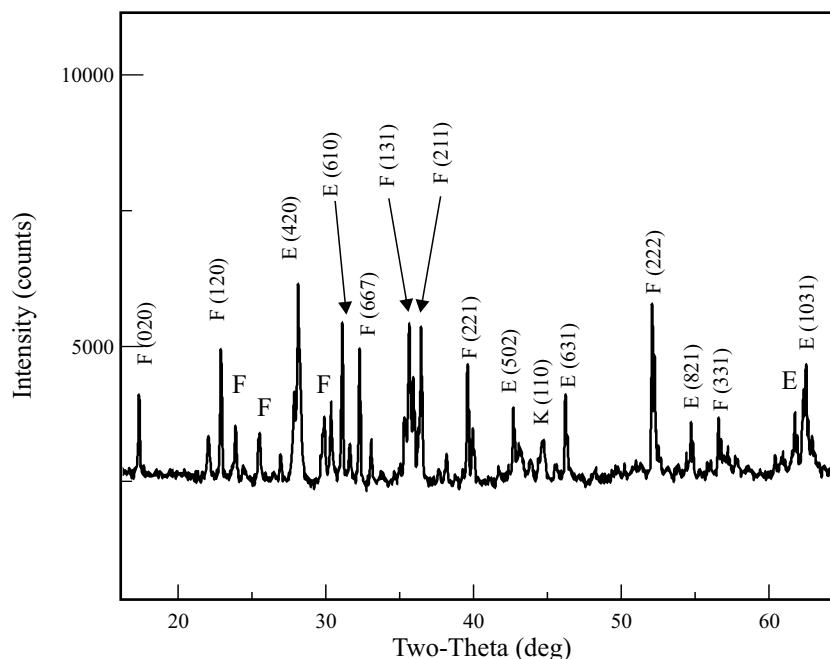
Figure 9. X-ray diffraction pattern of powdered bulk sample of Escalón meteorite. F: forsterite, E: enstatite, K: kamacite.

for their olivines and ferrosilite with 16.5 mol % for their orthopyroxenes). The silicate mineral composition homogeneity and the well defined chondrule boundaries suggest that Escalón belongs to petrologic type 4 (classification of Van Schmus and Wood, 1967).

Kamacite Co concentrations vary systematically in the chondrite chemical groups; kamacite in H, L, LL group chondrites contain 0.4–0.5, 0.7–1.0, and 1.5–3 wt. % Co, respectively (Rubin, 1990; Reisener and Goldstein, 2003). The kamacite Co content (0.318–0.432) in Escalón meteorite is almost similar to H group chondrites.

There are no visible oxidation of metal or sulfide, and only a limonitic staining may be noticeable in transmitted light, which characterize a weathering grade W0, according to the classification scheme proposed by Wlotzka (1993) for ordinary chondrites.

The average diameter in Escalón chondrules of 0.62 mm is larger than normal for H chondrites, which show the smallest sizes among ordinary chondrite (Rubin, 2005). Possibly, chondrule precursors were larger or more densely distributed in the environment where this meteorite formed as part of a primitive asteroid.

Glass in Escalón is alkaline and similar to igneous rocks of the alkaline series (Figures 8a, 8b). Normative albite content is dominant and resemble that of other ordinary chondrites, in particular to Dimmitt H chondrite (Krot and Rubin, 1994). Glass in Escalón chondrules and matrix has the same composition, maybe because it is a quench product solidified at very high temperatures. According to Varela *et al.* (2006) all meteorite glasses are the result of an unique universal process, representing the remnants of the liquid that facilitated growth of crystals from primary

liquid condensation; they reasoned that, in contrast to mayor elements, trace element abundances of all glasses display the same pattern.

The opaque phases study is important because they registred the thermal histories of meteorites (Wood, 1967; Reisener and Goldstein, 2003). The spherical shape of metallic phases inside some silicate grains in Escalón (Figure 3e) indicate an origin as liquid droplets that may be interpreted as relicts of a primary solidification structure by the rapid, non-equilibrium cooling of the Fe-Ni-S melts to temperatures of about 700 °C, similar to some textures in Tieschitz meteorite (Bevan and Axon, 1980). The plessitic texture also observed in this chondrite, possibly was formed at low temperatures from the decomposition of high temperature taenite, which was retained during slow cooling (Brearley and Jones, 1998).

Zoned taenite has received much attention because the Ni profiles are useful for calculating metallographic cooling rates (Reisener and Goldstein, 2003). Tetrataenite, which forms by ordering of Fe and Ni atoms in taenite, makes rims around taenite grains in chondrites below 350 ºC and slow cooling (Clarke and Scott, 1980). Taenite in the Escalón meteorite shows the highest Ni content at the edge (±50 wt. %), and the lowest at the center (±30 wt.%) (Figure 4e).

The metallic Ni-Fe phases of this meteorite are typical of slowly-cooled ordinary chondrites. The kamacite is monocrystalline and has Neumann bands. Most of the zoned taenites are isolated from kamacite; larger zoned taenite grains have martensitic interiors. Tetrataenite, an ordered FeNi phase (Clarke and Scott, 1980), occurs at some kamacite borders, and also surrounds some of the zoned taenite

grains that are associated with troilite.

In ordinary chondrites, metallic copper is rare compared to metallic Fe-Ni alloy, and it occurs in several petrographic assemblages (Rubin, 1994); In Escalón, metallic Cu, 10-16 μm in size, occurs enclosed in metallic Fe-Ni (taenite), and it is adjacent to small irregular troilite grains inside taenite. This type of assemblage is reported as the most common occurrence in ordinary chondrites, and it may have formed by localized shock melting or remelting of a metal-troilite assemblage (Rubin, 1994).

Shock metamorphic effects on Escalón correspond to shock stage S3, based on the presence of planar fractures in olivine (not shown by all grains) and undulatory extinction in all olivine grains, irregular fractures, and the presence of thin opaque veins. The black color of the hand specimen can be the result of numerous fine-grained metallic Fe-Ni-troilite particles, which may be associated with the shock effects (Stöffler *et al.*, 1991). The other petrographic shock signatures in Escalón occur as chromite-plagioclase assemblages, and polycrystalline troilite, metallic Cu, Cr and Fe-Ni blebs inclusions in olivine are relict shock features, which are consistent with a history of shock and annealing (Rubin, 2003, 2004; Bennett and McSween, 1996).

Other H4 chondrite with similar characteristics to Escalón are Menow and Ste. Marguerite (Michel-Levy, 1981).

CONCLUSIONS

Escalón is a high iron chondrite (H) as indicated by the average olivine composition (Fa_{19}) and average composition of pyroxene ($Fs_{13.6-16.3}$).

Classification as petrologic type 4 is indicated by the readily discernible chondrules, modest recrystallization and the Wo content of low-Ca pyroxene, which is within the range of typical type 4 chondrites .

The occurrence of plessitic texture and tetrataenite points to a slow cooling at low temperature.

Growth steps were observed in olivine, pyroxene and troilite crystals, whereas shock effects determined in Escalón were undulatory extinction of most olivine grains, and the occurrence of planar fractures, as well as some opaque shock veins indicating stage 3 of Stöffler *et al.* (1991). Other petrographic shock indicators observed in Escalón and stated by Rubin (2004) in equilibrated ordinary chondrite include: chromite-plagioclase assemblages, polycrystalline troilite, metallic Cu and Fe-Ni blebs inclusions in olivine, confirming shock stage S3 for Escalón.

ACKNOWLEDGEMENTS

REFERENCES

Bennett, M.E., McSween, H.Y., 1996, Shock features in iron-nickel metal and troilite of L-group ordinary chondrites: Meteoritics & Planetary Science, 31, 255-264.

Bevan, A.W.R., Axon, H.J., 1980, Metallography and thermal history of the Tieschitz unequilibrated meteorite-metallic chondrules and the origin of polycrystalline taenite: Earth and Planetary Science Letters, 47, 353-360.

Brearley, A. J., Jones, R. H., 1998, Chondritic meteorites, *in* Papike J.J., (ed.), Planetary materials: Washington D.C., Mineralogical Society of America, Reviews in Mineralogy, 36, 3.1-3.398.

Bunch, T.E., Keil, K., Snetsinger, K.G., 1967, Chromite composition in relation to chemistry and texture of ordinary chondrites: Geochimica et Cosmochimica Acta, 31, 1568-1582.

Clarke, R.S., Scott, E.R.D., 1980, Tetrataenite-ordered FeNi, a new mineral in meteorites: American Mineralogist, 65, 624-630.

Grossman, J.N., Rubin, A.E., Nagahara H., King E.A., 1988, Properties of chondrules, *in* Kerridge, J.F., Matthews M.S. (eds.), Meteorites and the early solar system: Tucson, Arizona, U.S.A., University of. Arizona Press, 619-654.

Irvine, T.N., Baragar W.R.A., 1971, A guide to the chemical classification of the common volcanic rocks: Canadian Journal of Earth Science, 8, 523-548.

Krot, A., Rubin, A.E., 1994, Glass-rich chondrules in ordinary chondrites: Meteoritics & Planetary Science, 29, 697-707.

Krot, A.N., Keil, K., Goodrich, C.A., Scott, E.R.D., Weisberg, M.K., 2003, Classification of meteorites, *in* Davis A.M. (ed.), Meteorites, Comets and Planets: Oxford, Elsevier, Treatise on Geochemistry (Holland H.D., Turekian K.K., eds.), v. 1, 83-128.

Michel-Levy, M.C., 1981, Some clues to the history of the H-group chondrites: Earth and Planetary Science Letters, 54, 67-80.

Nehru, C.E., Weisberg, M.K., Prinz, M., 1997, Chromites in unequilibrated ordinary chondrites, *en* 28th Annual Lunar and Planetary Science Conference, 1651.PDF, 2 pp.

Reisener, R.J., Goldstein, J.I., 2003, Ordinary chondrite metallography, Part 2. Formation of zoned and unzoned metal particles in relatively unshocked H, L, and LL chondrites: Meteoritics & Planetary Science, 38, 1679-1696.

Rubin, A.E., 1990, Kamacite and olivine in ordinary chondrites: Intergroup and intragroup relationships: Geochimica et Cosmochimica Acta, 54, 1217-1232.

Rubin, A.E., 1992, A shock-metamorphic model for silicate darkening and compositionally Kamacite and olivine in ordinary chondrites: Intergroup and intragroup relationships: Geochimica et Cosmochimica Acta, 54, 1217-1232.

Rubin, A.E., 1994, Metallic copper in ordinary chondrites: Meteoritics & Planetary Science, 29, 93-98.

Rubin, A.E., 2003, Chromite-plagioclse assemblages as a new shock indicator; Implications for the schock and thermal histories of ordinary chondrites: Geochimica et Cosmochimica Acta, 67, 2695-2709.

Rubin, A.E., 2004, Post-shock annealing and post-annealing shock in equilibrated ordinary chondrites: implications for the thermal and schock histories of chondritic asteroids: Geochimica et Cosmochimica Acta, 68, 673-689.

Rubin, A.E., 2005, Relationships among intrinsic properties of ordinary chondrites: Oxidation state, bulk chemistry oxygen-isotopic composition, petrologic type and chondrule size: Geochimica et Cosmochimica Acta, 69(20), 4907-4918.

Sánchez-Rubio, G., Rubinovich-Kogan, R., Lozano-Santa Cruz, R., Medina-Malagón, S., Flores-Gutiérrez, D., 2001, Las Meteoritas de México: México, Universidad Nacional Autónoma de México, Instituto de Geología, Instituto de Geofísica e Instituto de Astronomía, 85 pp.

Scott, E.R.D., Krot, A.N., 2003, Chondrites and their components, *in* Davis, A.M. (ed.), Meteorites, Comets and Planets: Oxford, Elsevier, Treatise on Geochemistry, (Holland H.D., Turekian K.K., eds.), v. 1, 143-200.

Scott, E.R., Taylor, G.J., Keil, K., 1986, Accretion, metamorphism and brecciation of ordinary chondrites: Evidence from petrologic studies of meteorites from Rooselvet County, New Mexico, *in* Procedings of the 17th Lunar and Planetary Science Conference, Part 1: Journal of Geophysical Research, 91(B13), E115-E123.

Stöffler, D., Keil, K., Scott, E.R.D., 1991, Shock metamorphism of ordinary chondrites: Geochimica et Cosmochimica Acta, 55, 3845-3867.

Van Schmus, W.R., Ribbe, P.H., 1968, The composition and structural state of feldspar from chondritic meteorites: Geochimica et Cosmochimica Acta, 32, 1327-1342.

Van Schmus, W.R., Wood, J.A., 1967, A chemical-petrologic classification for the chondritic meteorites: Geochimica et Cosmochimica Acta, 31(5), 747-765.

Varela, M.E., Kurat, G., 2006, An universal meteorite formation process (resumen), *en* 69th Meeting of the Meteoritical Society: Meteoritics & Planetary Science, 41(suppl.), p. A180.

Yabuki, H., Goresy, A., 1986, Phosphate-bearing microspherules in chondrules of unequilibrated ordinary chondrite, *in* Proceedings of the Tenth Symposium on Antartic Meteorites: Tokyo, National Institute of Polar Research, Memoirs, Special Issue 4, 235-242.

Wlotzka, F., 1993, A weathering scale for the ordinary chondrites (resumen): Meteoritics & Planetary Science, 23, 312.

Wlotzka F. 1994, The Meteoritical Bulletin, No. 77: Meteoritics & Planetary Science, 29, 891-897.

Wood, J.A., 1967, Chondrites: Their metallic minerals, thermal histories, and parent bodies: Icarus,6, 1-49.